

Investigating the Binding Behavior of CEP-37440 with Human Serum Albumin Using Multi-Spectroscopy and Molecular Docking

Ahmed Hassan Bakheit, Hatim
M. Eissa, Ayman Alkhider, K.
Murwan SabahelKhier, Omer
Abdalla Ahmed Hamdi

Al-Neelain University

GC-NU Journal

ISSN :1858-6228

Volume 17-2022
Issue 3



Graduate college
Al-Neelain University

Investigating the Binding Behavior of CEP-37440 with Human Serum Albumin Using Multi-Spectroscopy and Molecular Docking

Ahmed Hassan Bakheit^{1*}, Hatim M. Eissa¹, Ayman Alkhider¹, K. Murwan SabahelKhier², Omer Abdalla Ahmed Hamdia¹

Department of Chemistry, Faculty of Sciences and Technology, Al-Neelain University, Khartoum, Sudan

²Department of Biochemistry and Molecular Biology, Faculty of Sciences and Technology, Al-Neelain University, Khartoum, Sudan

*Corresponding author E-mail:

Abstract

CEP-37440 is an orally administered dual kinase inhibitor of Anaplastic lymphoma kinase (ALK) and focal adhesion kinase (FAK) with potential anticancer action. Human serum albumin, often known as HSA, is a vital transport protein that delivers hormones and a number of other compounds to the location in the body where they are supposed to have their effect. Fluorescence spectra were used to explore the interaction between CEP and Human Serum Albumin (HSA), a putative carrier of this medication in vivo. A shift in the intrinsic fluorescence was observable as a direct consequence of the association process. According to two models provided by Stern-Volmer and Scatchard equations, the emission spectra were studied to determine the association constant (K_b) values in the following different temperature 298, 303, and 310 K. and (pH 7.4). The results indicate that the association constants were sensitive to temperature changes. At 25°C, the value of K_b was $4.2169 \times 10^4 \text{ M}^{-1}$. In addition, the thermodynamic parameters for the interaction between HSA and CEP, namely the enthalpy change (ΔH) and the entropy change (ΔS), were calculated using Van't Hoff plots to be $-47,307 \text{ kJ/mol}$ and $247,266 \text{ J/mol}\cdot\text{K}$, respectively. According to the results of the thermodynamic study of the process by which the HSA-CEP complex was formed, the process of binding was enthalpically and entropically driven, as well as spontaneous, and electrostatic interaction is the primary intermolecular force responsible for maintaining the stability of the complex, that results agree with molecular docking studies. The results of the molecular docking and competitive displacement studies showed that CEP binds to HSA subdomain IIA preferentially..

Keywords: CEP-37440; Human Serum Albumin (HSA); synchronous fluorescence; 3D fluorescence; static fluorescence quenching; FRET; molecular docking.

Introduction

CEP-37440 (figure 1-(A)), also known as the ALK-FAK Inhibitor, is a dual kinase inhibitor that may be taken orally. It inhibits the receptor tyrosine kinase anaplastic lymphoma kinase (ALK) as well as the focal adhesion kinase (FAK), and it has the potential to prevent the growth of tumours. Once administered, CEP-37440 selectively binds to and inhibits both ALK and FAK kinases. The inhibition disrupts ALK-and FAK-mediated signal transduction pathways, subsequently inhibiting tumour cell proliferation in ALK and FAK overexpressing tumour cells. The inhibition disrupts ALK- and FAK-mediated signal transduction pathways, subsequently inhibiting tumour cell proliferation in ALK- and FAK-overexpressing tumour cells.

ALK is a member of the insulin receptor superfamily and plays a key part in the development of the nervous system. Its dysregulation and the rearrangement of its genes are related with a wide variety of cancer cells. The cytoplasmic tyrosine kinase FAK is a signal transducer for integrins; it is increased and constitutively active in numerous types of tumours; it plays an important role in tumour cell motility, proliferation, survival, and tumour angiogenesis (Bian et al., 2004).

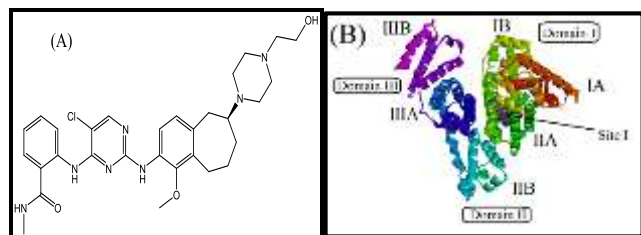


Figure 1: (A) chemical structure of CEP; (B) molecular structure of HSA.

Recent research (Sugio *et al.*, 1999, Wu and Stryer, 1972, Saber Abdelhameed *et al.*, 2022, Alanazi *et al.*, 2021) has been conducted to investigate the understanding of binding affinity and the mechanism of plasma proteins and drug interactions. Recent advances in nanotechnology have enabled the study of interaction processes (Dufour and Dangles, 2005, Lakowicz, 2006). The pharmacodynamic and pharmacokinetic features of therapeutic medications in the human system are profoundly influenced by the interaction between the drug proteins (plasma) and their mechanism (Alanazi *et al.*, 2021). In addition, the interactions between pharmaceuticals and plasma proteins are helpful in determining the therapeutic efficacy, distribution, and bioavailability of therapeutic medications. These interactions also contribute to the enhancement of solubility in plasma protein, the reduction of toxicity, and the protection against oxidation (Chamani and Heshmati, 2008, Marouzi *et al.*, 2017).

Human serum albumin (HSA) is a major plasma protein that supports the transfer of several compounds and metabolites (Figure 1B) (He and Carter, 1992). The three-dimensional structure of this protein, which is found in plasma, consists of three homologous domains and reveals that it is a monomeric chain globular protein with 585 amino acid residues (I-III-A and B subdomains). Sudlow's site I (subdomains IIA) and Sudlow's site II (subdomains IIIA) are the important drug-binding areas in the HSA (Qi *et al.*, 2016, Carballal *et al.*, 2003). On the other hand, there is another site known as Site III (subdomain IB), which is also thought to play an important part in the process of binding a variety of medicines (Carballal *et al.*, 2003). As a result, HSA possesses many binding sites and the capacity to bind a variety of medications, which enables it to operate as an essential component of a drug carrier (Rabbani *et al.*, 2018).

In addition, the binding of medicinal medicines to HSA is frequently reversible using weak interactions including as hydrogen bonds, hydrophobic forces, ionic contacts, and van der Waal's interactions (Alam *et al.*, 2018).

Binding mechanisms between CEP and HSA have not been studied to our knowledge. Under physiological settings, multi-spectroscopic methods and biochemical and molecular docking methodologies were used to investigate the binding characteristics of CEP with HSA. To investigate the pharmacodynamics and pharmacokinetics of CEP, however, we examined the possibility of complexation between CEP and HSA. The interactions between CEP and HSA that have been documented here would explain the process of binding at the molecular level and help attempts to adapt novel therapeutic medicines in order to improve their distribution inside the human body.

Results and Discussion

UV-Vis Absorption Spectroscopy

In order to examine the structural and conformational changes in the protein molecule that are produced by the binding ligands, UV-Vis spectral investigations are carried out. This method provides insights into the interaction mechanisms between the two entities (Zhao *et al.*, 2010). Figure 2 (A) & (B) depicts the UV-Vis absorption spectra of HSA and HSA-CEP complex. From the spectra, it is clear that HSA has an absorption peak at 280 nm, which is caused by the π - π^* transition of aromatic amino acids (tryptophan (W), tyrosine (Y), and phenylalanine) (Lakowicz, 2006). The absorption wavelength shifted somewhat with increasing CEP concentration. This blue shift is evidence that CEP binding is linked to modifications in the immediate surroundings of HSA. In addition, there is a rise in UV-absorption intensities of HSA at about 280 nm with increasing quantities of CEP, and this hyperchromicity implies the establishment of the HSA-CEP system. Hyperchromism at around 280 nm in HSA following the addition of CEP demonstrates that the aromatic amino acid (W and Y) microenvironment changes as a result of the development of the HSA-CEP complex (Kandagal *et al.*, 2006, Peng *et al.*, 2015).

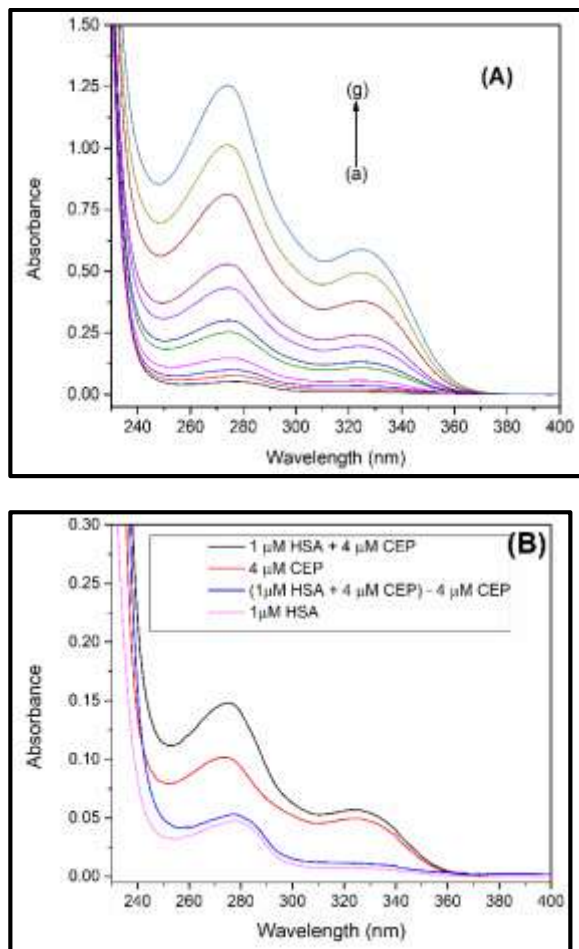


Figure 2. UV-vis absorption spectra of HSA in presence and absence of CEP at 298 K. HSA concentration was fixed at 1 μM (a), while that of CEP was varied from 1, 2, 4, 6, 8, 10, and 15 μM (b-g). (B) UV-vis spectra of CEP, HSA and the formed complex with the normalized/corrected HSA-CEP spectrum (subtracted HSA, 1 μM).

Evaluation of FRET

FRET is a process involving the energy transfer between two chromophores that is dependent on their binding distance. In the course of the interaction between the ligand and the protein, the excitation energy is transferred from the donor to the acceptor. Therefore, the donor molecule no longer produces photons. The following are the criteria required for this energy transfer to take place: The molecule may produce fluorescence as an energy donor; the emission spectra of the donor overlaps with the absorption spectrum of the acceptor; and the distance between the donor and acceptor is smaller than 8 nm (Wu and Stryer, 1972).

The following formula may be used to calculate the efficiency of energy transfer (E) based on FRET data as follows:

$$E = 1 - \frac{F}{F_0} = \frac{R_0^6}{R_0^6 + r^6}, \quad (1)$$

where F and F_0 represent the fluorescence intensities of the donor molecule before and after interaction with the receptor molecule, r represents the distance between the donor and the receptor, and R_0 is the critical distance at E = 50%, which may be calculated using the following formula:

$$R_0^6 = 9.78 \times 10^3 (k^2 N^{-4} \Phi J(\lambda))^{\frac{1}{6}} \quad (\text{in } \text{\AA}), \quad (2)$$

Where Φ is the fluorescence quantum yield of the donor (0.15), N represents the refractive index of the medium (1,336), k^2 represents the spatial orientation factor of the dipole (2/3) and J represents the integral of the overlap between the fluorescence emission spectra of the donor and absorption spectra of the acceptor. J is provided by:

$$J = \frac{\sum F(\lambda) \varepsilon(\lambda) \lambda^4 \Delta\lambda}{\sum F(\lambda) \Delta\lambda}, \quad (3)$$

Figure 3 displays the overlapping spectrum that was formed when the emission spectra of HSA and the absorption spectrum of CEP were overlapped on one other. The J value that was calculated from this superposition was $6.72120510^{-15} \text{ cm}^3 \text{ L/mol}$. The values for E, R_0 , and r that were arrived at by calculation were $3.094627 \times 10^{22} \text{ k}_{\text{trans}}^{-1} \text{ s}^{-1}$, 2.3873 nm, and 2.3885 nm, respectively. The results showed that non-radiative energy transfer occurred between HSA and CEP because r was smaller than 8 nm. In furthermore, it could be further confirmed that CEP quenched HSA fluorescence in the same manner as the static quenching that occurs when r is greater than R_0 .

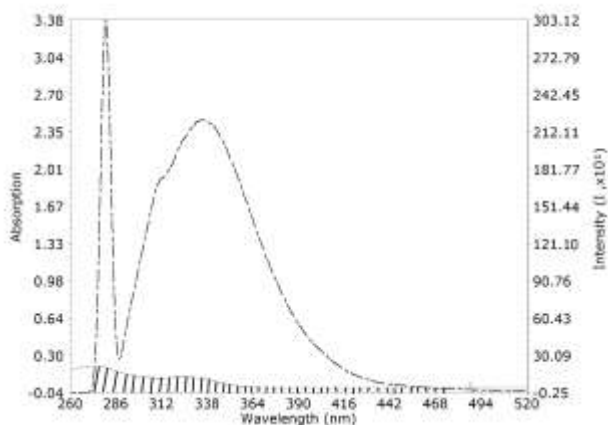


Figure 3: Overlap of fluorescence spectrum of HAS (a) and absorbance spectrum of CEP (b) ([HSA]: [CEP] = 1:1)

Investigating the HSA-CEP Complex Using Fluorescence Emission Spectroscopy

Fluorescence emission spectroscopy is a versatile biophysical method that is used to explore the binding mechanism of protein-ligand interactions and to analyse the binding characteristics. (Almehizia *et al.*, 2020, Kou *et al.*, 2021) Figure 4 illustrates both the fluorescence emission spectra of the HSA molecule by itself as well as the HSA-CEP complex. Due to the W-214 residue, it is evident from Figure 4 that HSA produces a significant emission peak at 340 nm when excited at 280 nm. Moreover, the addition of varying concentrations of CEP (0–15 M) quenching the fluorescence intensity of HSA with small altering the peak. This fluorescence suppression implies the establishment of the HSA-CEP system and a potential microenvironmental change in HSA upon treatment with CEP (Kameníková *et al.*, 2017, Tayyab *et al.*, 2020).

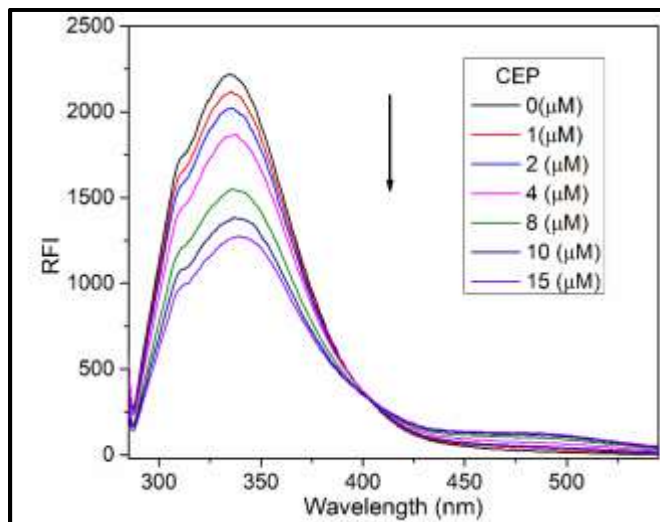


Figure 4. In the absence and presence of increasing concentrations of CEP, steady-state fluorescence emission spectra of HSA were observed. After excitation at 280 nm, the intrinsic fluorescence of the HSA was measured in the wavelength range of 285–545 nm at 298 K

The Fluorescence Quenching Mechanism (FQM) of the HSA-CEP System Interactions

Literature suggests that both dynamic and static quenching contribute to the protein's fluorescence quenching mechanism (FQM). In the process of dynamic quenching, the interaction between the fluorophore and the quencher is performed in an indirect fashion. On the other hand, when it comes to the phenomenon of static quenching, there is a ground state complex formation that takes place between the quencher and the fluorophore (Lakowicz, 2006). Consequently, the FQM may be separated according to their temperature dependency. In addition to this, the values of K_{sv} are inversely proportional to temperature in the case of static quenching, but in the event of dynamic quenching, the values are directly proportional to temperature. Therefore, the FQM of the HSA-CEP system was analyzed by acquiring the fluorescence spectra of HSA-CEP at various temperatures (295, 300, and 305 K). The fluorescence quenching data of the HSA-CEP system was then analysed using the Stern-Volmer equation (Lakowicz, 2006):

$$\frac{F_0}{F} = 1 + K_{SV}[Q], \quad (4)$$

where the steady-state fluorescence of HSA and the HSA-CEP complex, respectively, are represented by F_0 and F , respectively. K_{sv} stands for the Stern-Volmer constant, while $[Q]$ denotes the quencher concentration (CEP). Figure 5 illustrates the K_{sv} plot that was produced for the HSA-CEP system at three different temperatures: 295, 300, and 305 K. It was discovered that the K_{sv} values for the HSA-CEP system reduced as the temperature increases, which confirmed that the HSA-CEP system utilised a static quenching mechanism (Table 1).

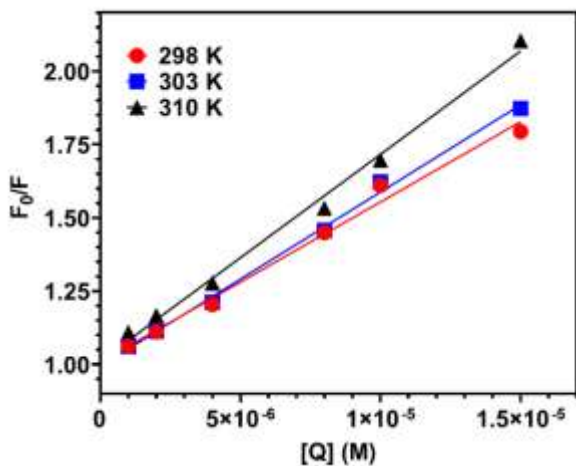


Table 1: The Stern-Volmer constant and quenching rate constant values for the CEP-HSA system.

T (K)	The Stern–Volmer equation from Figure 5			$K_{SV} \times 10^4 \text{ (M}^{-1}\text{)}$	$K_q \times 10^{11} \text{ (M}^{-1} \text{s}^{-1}\text{)}$
	Slope	Intercept	r^{2a}		
293	54691 ± 2924	1.007 ± 0.02417	0.9887	5.4691 ± 0.2924	9.12
298	59426 ± 1824	0.9938 ± 0.01508	0.9962	5.9426 ± 0.1824	9.90
303	70455 ± 2857	1.012 ± 0.02362	0.9935	7.0455 ± 0.2857	11.7

The Number of Binding Sites and Binding Constants in the HSA-CEP System

The HSA-CEP binding constant (K_b) and binding stoichiometry (n) were calculated from intrinsic fluorescence data collected at three different temperatures (295, 300, and 305 K) using the following equation (Lakowicz, 2006):

$$\log\left(\frac{F_0 - F}{F}\right) = \log K_a + n \log(Q), \quad (6)$$

Figure 5: Stern–Volmer plots demonstrating the binding of CEP to HSA at 288 K, 298 K, and 308 K

In addition, the fluorescence process, known as quenching, was investigated according to the values of the bimolecular rate constants, using an equation that went as follows:

$$K_Q = \frac{K_{SV}}{\tau_0}, \quad (5)$$

where k_q is the bimolecular rate constant and τ_0 is the average lifetime of the protein in the absence of the quencher, which for biopolymers is calculated to be 10^{-8} (Lakowicz and Weber, 1973). Table 1 presents the computed bimolecular quenching rate constant for the HSA-CEP system. The k_q values were discovered to be greater than the scattering collision constant ($2 \times 10^{10} \text{ M}^{-1} \text{ s}^{-1}$), which again indicates the presence of a static quenching mechanism between the HSA-CEP system (Shahabadi *et al.*, 2015).

Where the fluorescence intensities of the HSA with and without the quencher (CEP) are represented by F_0 and F , respectively. In the HSA-CEP system, the binding constant and the binding stoichiometry are represented by the symbols K_b and n respectively. For the purpose of determining the binding constant and the binding stoichiometry, the double log plot of $\log [(F_0 - F)/F]$ vs. $\log [Q]$ (Figure 6) was utilised. As can be seen in Figure

6, the values of K_b and n were derived from the plot by using the intercept and the slope of the curve. In accordance with Figure 6, the values of K_b and n for the HSA-CEP system are shown in Table 2 at a variety of temperatures. For the HSA-CEP system, a reduction in the binding constant was seen when temperatures were decreased. In addition, the binding constants were less than $\sim 10^4$, which indicates that HSA and CEP had a modest level of interaction.

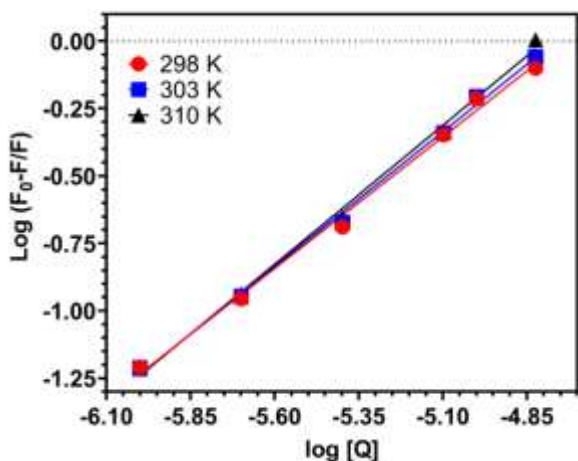


Figure 6. Graphs viewing $\log((F_0-F)/F)$ vs $\log[Q]$ for the native HSA system. The concentration of HSA was $4\mu\text{M}$, whereas the concentration of CEP ranged from 0 to $15\mu\text{M}$.

Analysis of the Thermodynamics of HSA and CEP Interactions to Determine the Binding Forces

The thermodynamic parameters were used to predict the major binding intermolecular forces involved in drug-protein interactions. The protein-drug interactions are bound together by van der Waal interactions, electrostatic forces, van der Waal interactions, and hydrophobic interactions. In addition, the sign and amount of the change in enthalpy (ΔH^0) and entropy (ΔS^0) are what determine the nature of the binding forces that are present in the drug-protein complex. When it comes to the hydrophobic interactions, both the sign and the magnitude of ΔH^0 and ΔS^0 need to have a value that is positive. Furthermore, it must be negative for ΔH^0 and ΔS^0 in the case of van der Waals forces

and hydrogen bonding (Jafari *et al.*, 2018, Shahabadi *et al.*, 2015). Moreover, for electrostatic interaction, ΔH^0 must be negative and ΔS^0 must be positive. The change in free energy (ΔG^0) of the HSA-CEP system may be calculated using the van't Hoff equation and the following thermodynamic equation:

$$\ln K_b = -\frac{\Delta H^0}{RT} + \frac{\Delta S^0}{R} \quad (7)$$

$$\Delta G^0 = \Delta H^0 - T\Delta S^0 \quad (8)$$

where R is the gas constant, which is $8.314 \text{ J mol}^{-1} \text{ K}^{-1}$, T denotes the temperature in kelvins, and K_b denotes the binding constant at each of the three temperatures that were studied. ΔH^0 and ΔS^0 are derived from the slope and intercept of the plot of $\ln K$ and $1/T$. (Figure 7).

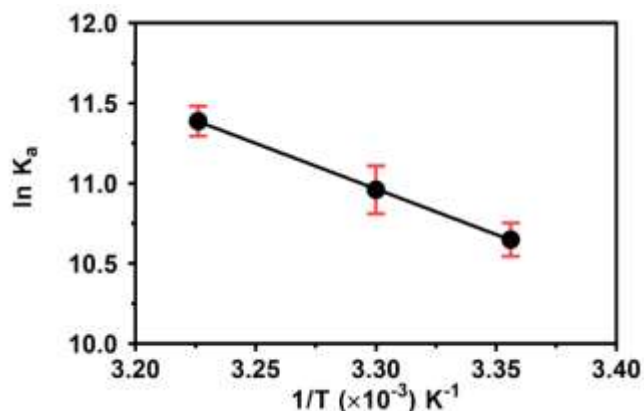


Figure 7: Van't Hof graphic illustrating the interaction of HSA ($[\text{HSA}] = 1.0 \mu\text{M}$) with CEP concentrations (ranging from 0.0 to $15.00 \mu\text{M}$) at each of the three temperatures.

Table 2 provides a summary of the findings about ΔG^0 , ΔH^0 , and ΔS^0 that were acquired from the interactions between HSA and CEP. Negative values for ΔH^0 and Positive values for ΔS^0 in the HSA-CEP system indicate that electrostatic interaction played a key role in the binding of CEP to HSA. Therefore, the synthesis of the HSA-CEP complex was exothermic reaction and occurred spontaneously (Ross and Subramanian, 1981).

Table 2: Binding parameters of HSA with CEP.

T (K)				The Van't Hoff Equation from Figure 7			
	Slope (n)	Intercept (logK _a)	r ^{2a}	K _b (M ⁻¹)	ΔG ⁰ (kJ mol ⁻¹)	ΔH ⁰ (kJ mol ⁻¹)	ΔS ⁰ (J mol ⁻¹ K ⁻¹)
293	0.9766	4.625± 0.166	0.9949	4.2169 x 10 ⁴	-49.78	-47.307	247.26
298	0.9994	4.761± 0.151	0.9968	5.7676 x 10 ⁴	-49.83		
303	1.031	4.946± 0.160	0.9966	8.8307 x 10 ⁴	-49.88		

Experiment using Synchronous Fluorescence Spectroscopy (SFS)

When proteins interact with ligands, synchronous fluorescence spectrometry can help offer information about the immediate environment of proteins surrounding W and Y residues (Vieira *et al.*, 2020, Lloyd, 1971). The difference in wavelength between the excitation and emission wavelengths of fluorescence in this experiment is representative of the characteristics of the spectra. (Y) residues have a wavelength difference ($\Delta\lambda$) of 15 nm, while (W) residues have a wavelength difference of 60 nm. Therefore, any change in the maximum emission wavelength reflects changes in the immediate environment around aromatic amino acid residues (Y and W). Figure 8 A,B depicts the SFS emission spectra of the HSA-CEP complex. It was evident from Figure 6 that the addition of CEP reduces the HSA fluorescence intensity of both (W and Y). In addition, neither of the spectra at $\Delta\lambda= 15$ nm nor 60 nm revealed any change in the emission wavelength. The interaction between HSA and CEP had no effect on the microenvironment of the protein molecule

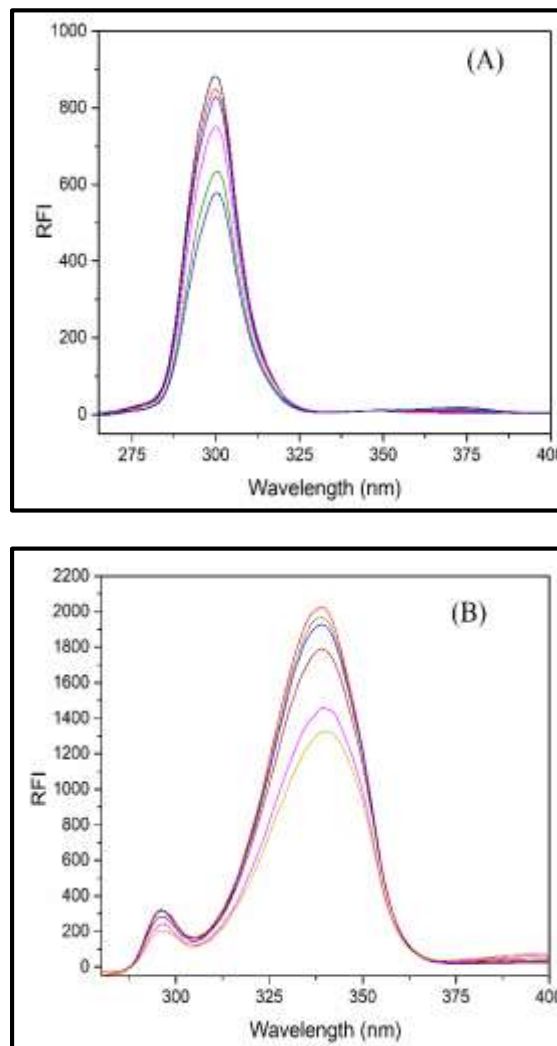


Figure 8: Synchronous fluorescence spectra of HSA after the addition of CEP at 298 K for (A) =15 nm and (B) =60 nm. HSA

= 1 μM; concentration of CEP curves at 0, 1, 2, 4, 8, 10, and 15 μM.

Prediction of Site Markers and binding constant in the HSA-CEP

According to Sudlow's categorization of binding sites, displacement studies were carried out on HSA to determine the specificity of CEP binding sites utilising site-selective probes such as warfarin (site I) and ibuprofen (site II) (Chen *et al.*, 2008). These studies were carried out to identify the specificity of CEP binding sites. The fluorescence measurements were utilised to determine the binding constants in the presence of the site probes. Equation (6) served as the basis for this calculation. Table 3 displays the CEP–HSA binding constants that occur when a number of different site probes are present. It is clear from looking at Table 3 that the CEP and the PHB compete with one another for site I on the Sudlow protein. Because of this, the binding constant got smaller as a result. Ibuprofen, on the other hand, did not significantly displace CEP in any appreciable way. As a consequence of this, it is anticipated that site I within

subdomain IIA of HSA would function as the principal binding site for CEP, as shown in figure 9.

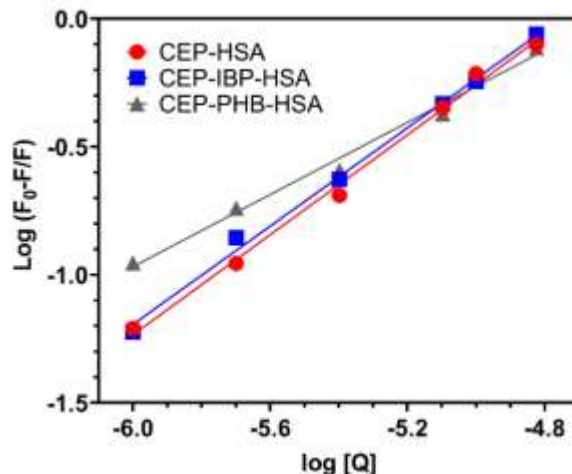


Figure 9: Graphs of $\log((F_0-F)/F)$ vs $\log[Q]$ for the HSA site probe system. HSA and site probe (ibuprofen and phenylbutazone) concentrations were 8 μM and 2.0 μM, respectively, whereas CEL concentrations ranged from 0 to 15 μM.

Table 3. The comparison of binding constants of CEP-HSA before and after the addition of site probe at 298 K.

Systems	Intercept ($\log K_b$)	Binding constants (L/mol)	Slope (n)	r ²
HSA+CEP	4.625±0.186	4.2169x10 ⁴	0.9766±0.0348	0.9949
HSA+CEP+Ibuprofen	4.566±0.161	3.6812x10 ⁴	0.960±0.0302	0.9961
HSA+CEP+Phenylbutazone	3.257±0.202	1.8072x10 ³	0.7042±0.0378	0.9886

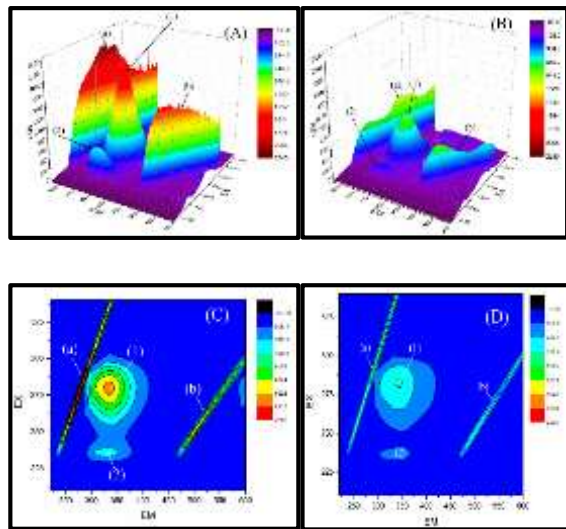
Three-dimensional fluorescence spectra (3-DFSs)

The 3-DFSs of HSA with and without CEP were calculated and depicted in Fig. 10 (A, B, C and D) in order to gather more information on the change in HSA conformation following interaction with CEP. Four different peaks with the designations 1, 2, a, and b exist. Peak a, the Rayleigh scattering peak ($\lambda_{em} = \lambda_{ex}$), indicates the fluorescence features of polypeptide backbone structures. Peak b, the second-order scattering ($\lambda_{em} = 2\lambda_{ex}$), is a

typical fluorescence peak induced by tyrosine or tryptophan residues (Zhang *et al.*, 2008), whereas Peak 1 ($\lambda_{ex}/\lambda_{em} = 278/340$

nm) is excited at a wavelength of around 280 nm. Fluorescence is emitted by Trp and Tyr residues in HSA at peak 2 ($\lambda_{ex}/\lambda_{em} = 226/340$ nm), which was primarily driven by the transition of $n \rightarrow \pi^*$ of the characteristic C=O in the polypeptide backbone (Glazer and Smith, 1961). As seen in figure 11, the intensities of Peaks 1 and 2 dropped as CEP was gradually added to HSA

solutions. These data suggested that the HSA-CEP complex would be formed when CEP associated to HAS (Shi *et al.*, 2018).



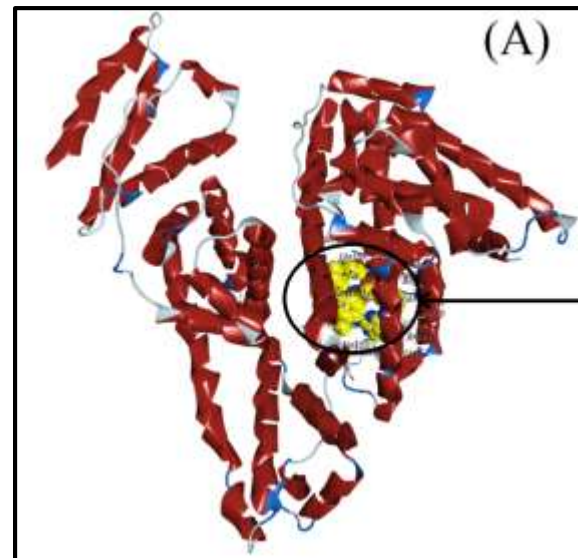
Figure

10: 3D-fluorescence spectra and contour diagrams of (A) & (C) HSA and (B) & (D) HSA-CEP. The concentrations of HSA and CEP are set at 1 μ M and 10 μ M, respectively.

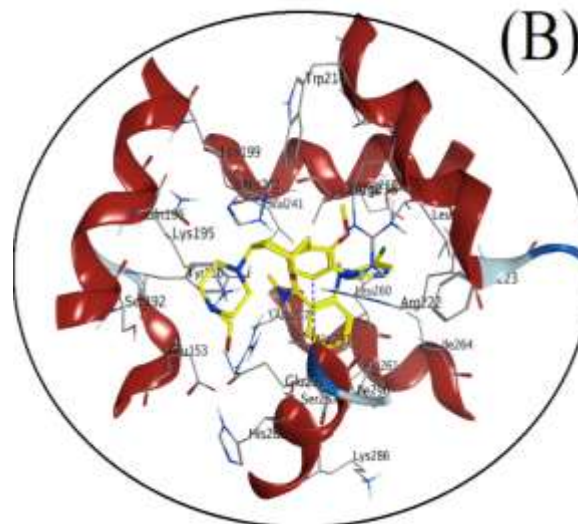
The HSA-CEP Complex: An Investigation Using Computational Models

Molecular docking study (Rabbani *et al.*, 2018, Moradi *et al.*, 2015) was used to analyse the binding area and amino acid residues involved in the interaction of CEP with HSA. Figure 11A and B depict the most suited confirmation of the HSA-CEP system. The results from molecular docking revealed that the CEP-binding region at subdomain IIA (Site I) of HSA (Figure 11 B). Additionally, CEP interacts to HSA and creates two hydrogen bonds with (ALA291, and GLU292 amino acid residues), as well as an electrostatic interaction with GLU292 of HSA (Figure 12). In addition to the two hydrogen bonds and electrostatic interaction, the CEP molecule is surrounded by various interactions with TYR150, GLU153, SER192, LYS195, LYS199, TRP214, ARG218, LEU219, ARG222, PHE223, LEU234, LEU238 VAL241, HIS242, ARG257, LEU260, ALA261, ILE264, SER287, HIS288, ILE290 (Figure 12). In addition, the MOE study indicate that the binding affinity of CEP to HSA was -9,012 kcal mol⁻¹. Thus, we may infer that the results

of molecular docking are consistent with those of investigations with siteI displacement markers (Figure 7).



Figure



11

(A): Docked position of the HSA with CEP illustrating binding at Sudlow site I (B) Expanded depiction of the interaction between CEP and amino acids at site I

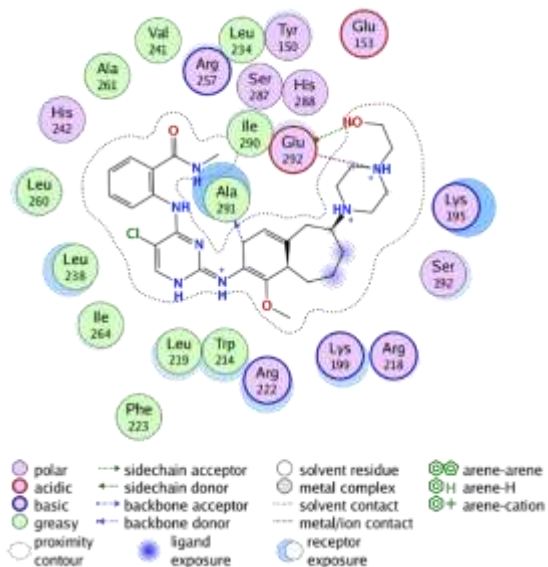


Figure 12. The 2D binding site was enlarged to reveal the amino acid residue around HSA that interacts with CEP.

Materials and Methods

Chemical & Reagents

The 99.97% pure CEP standard powder was acquired from MedChemExpress (Princeton, NJ, USA), whereas all of the chemicals, reagents, buffer ingredients, and solvent were purchased from Sigma-Aldrich Company. The HSA used in this study was a fraction V powder that did not include any fatty acids (St Louis, MO, USA). The whole investigation utilised double-distilled and deionized water from a Milli-Q® UF-Plus purification system (Millipore, Bedford, MA, USA).

Sample Preparation

A 50 μM HSA stock sample was dissolved in phosphate-buffered saline with a pH of 7.4. In addition, the stock of CEP (5 mM) was made in acetonitrile, and the standard stock of CEP samples was made by diluting the stock with PBS (phosphate-buffered saline), pH 7.4. Finally, Type I Millipore water was used to make the buffer (Burlington, MA, USA).

Instrumentations

The UV-Vis absorption spectra were obtained using a UV-1800 spectrophotometer (Shimadzu, Kyoto, Japan) by employing a 1.0 cm x 1.0 cm cell for the experiment. The fluorescence spectra were measured with a spectrofluorometer model number FP-8200 made by JASCO and located in Hachioji, Tokyo, Japan. The slit width of the instrument was 5 nm, and it was equipped with a quartz cell.

Methods

UV-Visible Absorption Spectroscopy

The UV-Visible absorbance spectra of HSA (1 μM) were acquired at 298 K at wavelengths ranging from 240 to 400 nm, and baseline correction was carried out with the use of an appropriate buffer. This was done in both the absence and presence of CEP (0–15 μM).

Steady-State Fluorescence Measurements

When excited at 280 nm, the fluorescence spectrum of HSA was measured at an emission wavelength of (290–520 nm). To estimate thermodynamic parameters, samples of HSA (1 μM) were titrated with CEP (0–15 μM) at three different temperatures (298, 303, and 310 K). The effects of the inner filter were taken into account when correcting the fluorescence data that was collected.

Synchronous Fluorescence Spectroscopy (SFS) Experiments

For the purpose of this experiment, SFS measurements of HSA (1 μM) were titrated with various concentrations of CEP (0–15 μM). These measurements were carried out in separate experiments using wavelength intervals ($\Delta\lambda$) of 15 nm for the tyrosine residue (Y) and 60 nm for the tryptophan residue (W) under the identical experimental conditions as the fluorescence measurements.

Competitive Site Probe Displacement (CSPD) Experiments

In short, in these experiments, CSPD tests were used to find the site on the HSA where CEP binds. We used the site markers phenylbutazon (PhB) (Sudlow's site I) and ibuprofen (IBP)

(Sudlow's site II) to find the part of HSA where CEP binds. At first, fluorescence spectra were made by titrating a solution of 1 μM HSA, and site markers (8 μM IBP, or 2 μM PhB) with increasing concentrations of CEP (0–15 μM) in different experiments. For the fluorescence measurements, all of the other parameters, like the wavelengths of excitation and emission, were the same.

Molecular Docking of HSA with CEP

The binding mechanism between CEP and HSA has been predicted using molecular docking and MOE. The HSA (PDB ID: 1BM0) and CEP (medchemexpress CEP-37440.html) molecular structures were acquired from Protein Data Bank (PDB) and medchemexpress, respectively. The highest-scoring conformations were chosen for interaction analysis. For docking analysis, MOE default settings were utilised.

Conclusions

In the present investigation, the binding interaction of the ALK-FAK inhibitor CEP with HSA was studied utilising spectroscopic, biochemical, and computational techniques. The findings of the CEP-HSA binding interactions demonstrated a moderate affinity of CEP for HSA. Additionally, both hydrogen bonding and hydrophobic interactions were found. The spectroscopic analyses indicate that CEP and HSA form a complex, and the system follows a static quenching process. In contrast, the thermodynamic characteristics of the HSA-CEP system computed using fluorescence spectroscopy at various temperatures reveal a spontaneous and exothermic reaction and suggest that are the major factors.

In addition, the results of the site-displacement experiment and molecular docking validate the CEP-binding area in subdomain IIA of HSA. This work is crucial and is anticipated to aid in the comprehension of the medication's processes and pharmacokinetics for future clinical research and innovative drug delivery methods.

Data Availability

On request, the corresponding author of this study will make the data that was used to support the conclusions of this study available to you.

Conflicts of Interest

The authors certify that there are no conflicting interests that might influence their work.

References

- ALAM, M. M., ABUL QAIS, F., AHMAD, I., ALAM, P., HASAN KHAN, R. & NASEEM, I. 2018. Multi-spectroscopic and molecular modelling approach to investigate the interaction of riboflavin with human serum albumin. *Journal of Biomolecular Structure and Dynamics*, 36, 795-809.
- ALANAZI, A. M., BAKHEIT, A. H., ATTWA, M. W. & ABDELHAMEED, A. S. 2021. Spectroscopic, molecular docking and dynamic simulation studies of binding between the new anticancer agent olmutinib and human serum albumin. *Journal of Biomolecular Structure and Dynamics*, 1-11.
- ALMEHIZIA, A. A., ALRABIAH, H., BAKHEIT, A. H., HASSAN, E. S., HERQASH, R. N. & ABDELHAMEED, A. S. 2020. Spectroscopic and molecular docking studies reveal binding characteristics of nazartinib (EGF816) to human serum albumin. *Royal Society open science*, 7, 191595.
- BIAN, Q., LIU, J., TIAN, J. & HU, Z. 2004. Binding of genistein to human serum albumin demonstrated using tryptophan fluorescence quenching. *International journal of biological macromolecules*, 34, 275-279.
- CARBALLAL, S., RADI, R., KIRK, M. C., BARNES, S., FREEMAN, B. A. & ALVAREZ, B. 2003. Sulfenic acid formation in human serum albumin by hydrogen peroxide and peroxyxynitrite. *Biochemistry*, 42, 9906-9914.
- CHAMANI, J. & HESHMATI, M. 2008. Mechanism for stabilization of the molten globule state of papain by sodium n-alkyl sulfates: spectroscopic and calorimetric

- approaches. *Journal of colloid and interface science*, 322, 119-127.
- CHEN, J., JIANG, X. Y., CHEN, X. Q. & CHEN, Y. 2008. Effect of temperature on the metronidazole–BSA interaction: multi-spectroscopic method. *Journal of Molecular Structure*, 876, 121-126.
- DUFOUR, C. & DANGLES, O. 2005. Flavonoid–serum albumin complexation: determination of binding constants and binding sites by fluorescence spectroscopy. *Biochimica et biophysica acta (BBA)-general subjects*, 1721, 164-173.
- GLAZER, A. & SMITH, E. L. 1961. Studies on the ultraviolet difference spectra of proteins and polypeptides. *J Biol Chem*, 236, 2942-2947.
- HE, X. M. & CARTER, D. C. 1992. Atomic structure and chemistry of human serum albumin. *Nature*, 358, 209-215.
- JAFARI, F., SAMADI, S., NOWROOZI, A., SADRJAVADI, K., MORADI, S., ASHRAFI-KOOSHK, M. R. & SHAHLAEI, M. 2018. Experimental and computational studies on the binding of diazinon to human serum albumin. *Journal of Biomolecular Structure and Dynamics*, 36, 1490-1510.
- KAMENÍKOVÁ, M., FURTMÜLLER, P. G., KLACSOVÁ, M., LOPEZ-GUZMAN, A., TOCA-HERRERA, J. L., VITKOVSKÁ, A., DEVÍNSKY, F., MUČAJI, P. & NAGY, M. 2017. Influence of quercetin on the interaction of glioclazide with human serum albumin–spectroscopic and docking approaches. *Luminescence*, 32, 1203-1211.
- KANDAGAL, P., ASHOKA, S., SEETHARAMAPPA, J., SHAIKH, S., JADEGOUD, Y. & IJARE, O. B. 2006. Study of the interaction of an anticancer drug with human and bovine serum albumin: spectroscopic approach. *Journal of pharmaceutical and biomedical analysis*, 41, 393-399.
- KOU, S.-B., LIN, Z.-Y., WANG, B.-L., SHI, J.-H. & LIU, Y.-X. 2021. Evaluation of the binding behavior of olmutinib (HM61713) with model transport protein: Insights from spectroscopic and molecular docking studies. *Journal of Molecular Structure*, 1224, 129024.
- LAKOWICZ, J. R. 2006. *Principles of fluorescence spectroscopy*, Springer.
- LAKOWICZ, J. R. & WEBER, G. 1973. Quenching of protein fluorescence by oxygen. Detection of structural fluctuations in proteins on the nanosecond time scale. *Biochemistry*, 12, 4171-4179.
- LLOYD, J. 1971. The nature and evidential value of the luminescence of automobile engine oils and related materials: Part I. Synchronous excitation of fluorescence emission. *Journal of the Forensic Science Society*, 11, 83-94.
- MAROUZI, S., RAD, A. S., BEIGOLI, S., BAGHAEI, P. T., DARBAN, R. A. & CHAMANI, J. 2017. Study on effect of lomefloxacin on human holo-transferrin in the presence of essential and nonessential amino acids: Spectroscopic and molecular modeling approaches. *International Journal of Biological Macromolecules*, 97, 688-699.
- MORADI, N., ASHRAFI-KOOSHK, M. R., GHOBADI, S., SHAHLAEI, M. & KHODARAHMI, R. 2015. Spectroscopic study of drug-binding characteristics of unmodified and pNPA-based acetylated human serum albumin: Does esterase activity affect microenvironment of drug binding sites on the protein? *Journal of Luminescence*, 160, 351-361.
- PENG, X., WANG, X., QI, W., HUANG, R., SU, R. & HE, Z. 2015. Deciphering the binding patterns and conformation changes upon the bovine serum albumin–rosmarinic acid complex. *Food & function*, 6, 2712-2726.
- QI, J., ZHANG, Y., GOU, Y., ZHANG, Z., ZHOU, Z., WU, X., YANG, F. & LIANG, H. 2016. Developing an anticancer copper (II) pro-drug based on the His242 residue of the human serum albumin carrier IIA subdomain. *Molecular pharmaceuticals*, 13, 1501-1507.
- RABBANI, G., LEE, E. J., AHMAD, K., BAIG, M. H. & CHOI, I. 2018. Binding of tolperisone hydrochloride with human serum albumin: effects on the conformation,

- thermodynamics, and activity of HSA. *Molecular pharmaceuticals*, 15, 1445-1456.
- ROSS, P. D. & SUBRAMANIAN, S. 1981. Thermodynamics of protein association reactions: forces contributing to stability. *Biochemistry*, 20, 3096-3102.
- SABER ABDELHAMEED, A., BAKHEIT, A. H., HASSAN, E. S., ALANAZI, A. M., NAGLAH, A. M. & ALRABIAH, H. 2022. Spectroscopic and computational investigation of the interaction between the new anticancer agent enasidenib and human serum albumin. *Spectrochimica Acta Part A: Molecular and Biomolecular Spectroscopy*, 270, 120790.
- SHAHABADI, N., HADIDI, S. & FEIZI, F. 2015. Study on the interaction of antiviral drug ‘Tenofovir’ with human serum albumin by spectral and molecular modeling methods. *Spectrochimica Acta Part A: Molecular and Biomolecular Spectroscopy*, 138, 169-175.
- SHI, J.-H., LOU, Y.-Y., ZHOU, K.-L. & PAN, D.-Q. 2018. Elucidation of intermolecular interaction of bovine serum albumin with Fenhexamid: a biophysical prospect. *Journal of Photochemistry and Photobiology B: Biology*, 180, 125-133.
- SUGIO, S., KASHIMA, A., MOCHIZUKI, S., NODA, M. & KOBAYASHI, K. 1999. Crystal structure of human serum albumin at 2.5 Å resolution. *Protein Engineering, Design and Selection*, 12, 439-446.
- TAYYAB, S., MIN, L. H., KABIR, M., KANDANDAPANI, S., RIDZWAN, N. F. W. & MOHAMAD, S. B. 2020. Exploring the interaction mechanism of a dicarboxamide fungicide, iprodione with bovine serum albumin. *Chemical Papers*, 74, 1633-1646.
- VIEIRA, T., STEVENS, A. C., CHTCHEMELININE, A., GAO, D., BADALOV, P. & HEUMANN, L. 2020. Development of a large-scale cyanation process using continuous flow chemistry en route to the synthesis of remdesivir. *Organic Process Research & Development*, 24, 2113-2121.
- WU, C.-W. & STRYER, L. 1972. Proximity relationships in rhodopsin. *Proceedings of the National Academy of Sciences*, 69, 1104-1108.
- ZHANG, Y.-Z., ZHOU, B., LIU, Y.-X., ZHOU, C.-X., DING, X.-L. & LIU, Y. 2008. Fluorescence study on the interaction of bovine serum albumin with p-aminoazobenzene. *Journal of fluorescence*, 18, 109-118.
- ZHAO, X., LIU, R., CHI, Z., TENG, Y. & QIN, P. 2010. New insights into the behavior of bovine serum albumin adsorbed onto carbon nanotubes: comprehensive spectroscopic studies. *The journal of physical chemistry B*, 114, 5625-5631.